

A Multi-Model Particle Filtering Algorithm for Indoor Tracking of Mobile Terminals Using RSS Data

Katrin Achutegui* Luca Martino* Javier Rodas† Carlos J. Escudero† Joaquín Míguez*

Abstract—In this paper we address the problem of indoor tracking using received signal strength (RSS) as a position-dependent data measurement. This type of measurements are very appealing because they can be easily obtained with a variety of wireless technologies which are relatively inexpensive. The extraction of accurate location information from RSS in indoor scenarios is not an easy task, though. Since RSS is highly influenced by multipath propagation, it turns out very hard to adequately model the correspondence between the received power and the transmitter-to-receiver distance. The measurement models proposed in the literature are site-specific and require a great deal of information regarding the structure of the building where the tracking will be performed and therefore are not useful for a general application. For that reason we propose the use of a compound model that combines several sub-models, whose parameters are adjusted to specific and different propagation environments. This methodology, called Interacting Multiple Models (IMM), has been used in the past for modeling the motion of maneuvering targets. Here, we extend its application to handle also the uncertainty in the RSS observations and we refer to the resulting state-space model as a generalized IMM (GIMM) system. The flexibility of the GIMM approach is attained at the expense of an increase in the number of random processes that must be accurately tracked. To overcome this difficulty, we introduce a Rao-Blackwellized sequential Monte Carlo tracking algorithm that exhibits good performance both with synthetic and experimental data.

I. INTRODUCTION

The problem of indoor navigation and tracking is currently receiving a great deal of attention because of its many practical applications, that include security, guidance, tourism and others. For this purpose, many types of position-dependent data can be exploited [1], [2], including times of arrival (ToA), time differences of arrival (TDoA), angles of arrival (AoA) or received signal strength (RSS). Although the latter is the most unstable type of range measurement that can be obtained (due to phenomena such as scattering or multipath propagation), the design of RSS-based location and tracking schemes is very appealing because they can be implemented using relatively inexpensive wireless network infrastructures. The difficulty to elaborate precise models of the RSS as a function of the distance between the transmitter and the receiver in indoor scenarios, however, has not been surmounted yet and, as a consequence, the design of RSS-based tracking algorithms which are both accurate and robust in practical environments remains an open problem [3].

In this paper, we propose a novel approach to indoor tracking using RSS that relies on

- (a) the representation of both the mobile target dynamics and the resulting RSS observations by means of multiple interacting models and
- (b) the sequential Monte Carlo (SMC) methodology [4] to recursively compute Bayesian estimates of the target position and velocity.

Interacting multiple-model (IMM) representations of the target dynamics have been used in the past to address the problem of maneuvering target tracking [5]. Our contribution in this work is to extend the notion of IMM to handle the uncertainty in *both* the dynamics *and* the RSS observations in a state-space random model. In particular, we allow the representation of the target motion and the RSS measurements to be drawn from a collection of candidate models according to a multivariate-indicator random process. We refer to the resulting state-space model as a generalized IMM (GIMM) system. The advantage of this scheme is that we can easily encompass a relatively broad range of indoor scenarios. Its main drawback is the need to track the target in a higher dimensional state space (its actual dimension depending on the number of interacting models used). We will show, however, that the SMC methodology, also known as particle filtering, is powerful enough to numerically compute accurate state estimates within this set up, in such a way that the former virtue is fully exploited while the latter limitation is overcome. We introduce a Rao-Blackwellized particle filtering algorithm in which a subset of the state variables is integrated out to improve the tracking accuracy.

The remaining of the paper is organized as follows. In Section II we describe the state space model that represents both the target dynamics and the associated indoor RSS measurements. In Section III we introduce the proposed particle filtering algorithm. Then, in Section IV we give a full account of the experimental setup constructed for the collection of real RSS data and show numerical results that illustrate the performance of the method. The paper is completed with some concluding remarks in Section V.

II. SYSTEM MODEL

A. Notation

Scalar magnitudes are denoted using regular face letters, e.g., x , while matrices and vectors are written as bold-face upper-case and lower-case letters, respectively, e.g., matrix \mathbf{X} and vector \mathbf{x} . We will use letter p to denote the true probability density function (pdf) of a random variable or vector. This is an argument-wise notation, common in Bayesian analysis. For two random variables x and y , $p(x)$ is the true pdf of x and

*Department of Signal Theory and Communications, Universidad Carlos III de Madrid (Spain). E-mail: {kachutegui,luca,jmiguez}@tsc.uc3m.es

†Department of Electronics and Systems, Universidade da Coruña (Spain). E-mail: {jrodas,escudero}@udc.es

$p(y)$ is the true pdf of y , possibly different. The conditional pdf of x given y is written $p(x|y)$. Exactly the same notation is used for probability mass functions (pmf's). Note that a pmf can be formally handled in the same way as a pdf by constructing it as a train of Dirac delta functions centered at the points where the probability masses are located.

B. Motion Models

It is common to model the motion of a target by means of a Markov stochastic process in discrete time [6]. Specifically, we formally represent the target dynamic state at time $t \in \mathbb{N}$ over a two dimensional region as a 2×1 complex vector $\mathbf{x}_{2,t} = [r_t \ v_t]^T \in \mathbb{C}^2$, where the complex scalars r_t and v_t provide the target position and velocity, respectively. The subscript ℓ in $\mathbf{x}_{\ell,t}$ is used to indicate the state vector dimension. Such a notation will prove useful as we later introduce extended versions of the state vector that incorporate additional state variables. A popular, due to its simplicity, dynamic model for $\mathbf{x}_{2,t}$ is the so-called ‘‘constant velocity’’ difference equation [6]

$$\underbrace{\begin{bmatrix} r_t \\ v_t \end{bmatrix}}_{\mathbf{x}_{2,t}} = \underbrace{\begin{bmatrix} 1 & T \\ 0 & 1 \end{bmatrix}}_{\mathbf{A}} \underbrace{\begin{bmatrix} r_{t-1} \\ v_{t-1} \end{bmatrix}}_{\mathbf{x}_{2,t-1}} + \underbrace{\begin{bmatrix} T^2/2 \\ T \end{bmatrix}}_{\mathbf{q}} u_t \quad (1)$$

where \mathbf{A} is a transition matrix that depends on the time-discretization period T , \mathbf{x}_{t-1} is the state vector in the previous time step and u_t is a complex Gaussian random variable with zero mean and variance σ_u^2 , denoted $u_t \sim CN(u_t; 0, \sigma_u^2)$. The noise term $\mathbf{q}u_t$ is a 2×1 complex Gaussian vector, with zero mean and covariance matrix $\sigma_u^2 \mathbf{q}\mathbf{q}^T$, that represents the effect of unknown accelerations.

While (1) yields a flexible model that enables the representation of a broad range of target trajectories, it does not exploit any specific features of the target motion that may be known before hand. In particular, it is relatively simple to extend (1) in order to capture the ability of the target to turn, i.e., to change the angle of the velocity v_t , that we denote as $\angle v_t$. Let $\omega_t \in \mathbb{R}$ denote the variation, in radians, of the angle of the velocity at time $t + 1$. Then we can write the 3×1 target state vector as $\mathbf{x}_{3,t} = [\omega_t, r_t, v_t]^T$, which evolves with time according to

$$\omega_t \sim p(\omega_t|\omega_{t-1})$$

$$\begin{bmatrix} r_t \\ v_t \end{bmatrix} = \underbrace{\begin{bmatrix} 1 & T \\ 0 & \exp(i\omega_{t-1}) \end{bmatrix}}_{\mathbf{A}(\omega_{t-1})} \underbrace{\begin{bmatrix} r_{t-1} \\ v_{t-1} \end{bmatrix}}_{\mathbf{x}_{2,t-1}} + \mathbf{q}u_t, \quad (2)$$

where $i = \sqrt{-1}$, the transition matrix $\mathbf{A}(\omega_{t-1})$ is a function of the turning angle and the conditional pdf $p(\omega_t|\omega_{t-1})$ is known. By selecting different distributions for ω_t one can devise different motion models. If the target may take any turn at any time, independently of its previous state, then $p(\omega_t|\omega_{t-1}) = p(\omega_t) = U([0, 2\pi])$, where $U(I)$ denotes the uniform density in the interval I . For some vehicles, the turning angle may be constrained to small angles, e.g., $p(\omega_t|\omega_{t-1}) = p(\omega_t) = U([0, \pi/4])$ or even restricted to discrete values, $p(\omega_t|\omega_{t-1}) = p(\omega_t) = U(\{\pm\pi/2\})$. It is also

possible to reduce the subset of turning angles as the velocity increases. We also note that in the degenerate case in which $\omega_t = 0$, with probability 1, for all t , then (2) reduces to (1).

Let us assume that, at a given time t , the target of interest may move according to one out of L motion models, indexed by the integers $\{1, 2, \dots, L\}$. Each motion model corresponds to a different transition pdf for the Markov process $\{\omega_t\}_{t \in \mathbb{N}}$. Therefore, in order to identify the specific densities, we introduce an additional state variable, denoted a_t . This is a discrete random indicator, $a_t \in \{1, \dots, L\}$, such that $a_{t-1} = l$ implies that ω_t is generated according to the l -th model. Thus, we need to write $\omega_t \sim p(\omega_t|\omega_{t-1}, a_{t-1})$ to make this dependence explicit. The conditional pmf $p(a_t|a_{t-1})$ is a part of the overall model and, therefore, assumed known.

By incorporating the indicator a_t to the target state, we obtain the 4×1 vector $\mathbf{x}_{4,t} = [a_t, \omega_t, r_t, v_t]^T$ which evolves according to the IMM equation

$$a_t \sim p(a_t|a_{t-1}), \quad \omega_t \sim p(\omega_t|\omega_{t-1}, a_{t-1})$$

$$\mathbf{x}_{2,t} = \mathbf{A}(\omega_{t-1})\mathbf{x}_{2,t-1} + \mathbf{q}u_t. \quad (3)$$

C. Measurement Models

We propose a scheme where RSS observations are collected from J sensors. The measurement provided by the j -th sensor at time t is denoted as $y_{j,t}$. The relationship between the observed RSS, $y_{j,t}$, and the target position, r_t , depends on the physical environment (obstacles, building materials, etc...) [3] and may change with time. In order to handle such uncertainty, we again use an IMM approach to model the data. Specifically, we allow the observation $y_{j,t}$ to be represented using one out of K different models. This is written as

$$y_{j,t} = f_{m_{j,t}}(r_t) + \varepsilon_{1,t}, \quad (4)$$

where $m_{j,t} \in \{1, \dots, K\}$ is a random index with known pmf $p(m_{j,t})$ that identifies the measurement model at time t for the j -th sensor, $f_{m_{j,t}}$ is the function used to represent the propagation conditions in the $m_{j,t}$ -th model, that determine the received RSS, and $\varepsilon_t \sim N(\varepsilon; 0, \sigma_\varepsilon^2)$ is normally distributed, zero-mean noise with variance σ_ε^2 (note the use of N for the density of a real Gaussian variable versus CN for a complex Gaussian). The form of each element in the collection of functions $\{f_1, f_2, \dots, f_K\}$ should be determined from field measurements collected in the scenarios where the tracking system may have to operate (which can be significantly different).

We write the measurement-model indicators together in the $J \times 1$ vector $\mathbf{m}_t = [m_{1,t}, \dots, m_{J,t}]^T$, hence the full target state has $J + 4$ components, $\mathbf{x}_{J+4,t} = [\mathbf{m}_t, a_t, \omega_t, r_t, v_t]^T$. The observations are put together in the $J \times 1$ vector $\mathbf{y}_t = [y_{1,t}, \dots, y_{J,t}]^T$. The indices in \mathbf{m}_t are assumed independent, but not necessarily identically distributed.

D. Summary

The generalized IMM (GIMM) state-space model that comprises L possible interacting submodels in the state equation and K submodels in the observation equation is described

by the set of relationships

$$\begin{aligned} \mathbf{m}_t &\sim p(\mathbf{m}_t), \quad a_t \sim p(a_t|a_{t-1}), \\ \boldsymbol{\omega}_t &\sim p(\boldsymbol{\omega}_t|\boldsymbol{\omega}_{t-1}, a_{t-1}), \quad \mathbf{x}_{2,t} = \mathbf{A}(\boldsymbol{\omega}_{t-1})\mathbf{x}_{2,t} + \mathbf{q}u_t, \\ \mathbf{y}_t &= \mathbf{f}(r_t, \mathbf{m}_t) + \boldsymbol{\varepsilon}_t, \end{aligned} \quad (5)$$

where $\mathbf{f}(r_t, \mathbf{m}_t) = [f_{m_{1,t}}(r_t), f_{m_{2,t}}(r_t), \dots, f_{m_{J,t}}(r_t)]^\top$ and $\boldsymbol{\varepsilon}_t = [\varepsilon_{1,t}, \dots, \varepsilon_{J,t}]^\top$, together with the prior pdf's $p(\boldsymbol{\omega}_0)$, $p(r_0)$ and $p(v_0)$ and the pmf $p(a_0)$. For the indoor tracking application, of interest in this paper, the goal is to accurately estimate the sequence of target positions, $r_{0:t} = \{r_0, r_1, \dots, r_t\}$, as time evolves. We tackle this problem using the SMC algorithm introduced in the next section.

III. TRACKING ALGORITHM

A. Sequential Monte Carlo Approximation

From a Bayesian point of view, the smoothing pdf

$$p(r_{0:t}, \boldsymbol{\omega}_{0:t}, a_{0:t} | \mathbf{y}_{1:t}) = \sum_{\mathbf{m}_{0:t}} \int_{v_{0:t}} p(\mathbf{x}_{J+4,0:t} | \mathbf{y}_{1:t}) dv_{0:t} \quad (6)$$

contains all relevant statistical information¹ for the estimation of $r_{0:t}$. The elimination of $v_{0:t}$ and $\mathbf{m}_{0:t}$ by marginalization is often termed Rao-Blackwellization and reduces the estimation variance [7], [8]. Unfortunately, the distribution of Eq. (6) cannot be obtained analytically and we have to resort to numerical approximation techniques. Our approach, in particular, is to build a point-mass approximation of $p(r_{0:t}, \boldsymbol{\omega}_{0:t}, a_{0:t} | \mathbf{y}_{1:t})$ consisting of M random samples in the space of $\{r_{0:t}, \boldsymbol{\omega}_{0:t}, a_{0:t}\}$, denoted $\{r_{0:t}^{(i)}, \boldsymbol{\omega}_{0:t}^{(i)}, a_{0:t}^{(i)}\}_{i=1}^M$, and associated importance weights, $\{w_t^{(i)}\}_{i=1}^M$. Each pair $\left\{ \left(r_{0:t}^{(i)}, \boldsymbol{\omega}_{0:t}^{(i)}, a_{0:t}^{(i)} \right), w_t^{(i)} \right\}$ is called a *particle* and we can use them to build the random measure

$$p_M(r_{0:t}, \boldsymbol{\omega}_{0:t}, a_{0:t} | \mathbf{y}_{1:t}) = \sum_{i=1}^M \delta_i(r_{0:t}, \boldsymbol{\omega}_{0:t}, a_{0:t}) w_t^{(i)}, \quad (7)$$

where δ_i is a delta measure located at $\left(r_{0:t}^{(i)}, \boldsymbol{\omega}_{0:t}^{(i)}, a_{0:t}^{(i)} \right)$ and the weights are assumed normalized, i.e., $\sum_{i=1}^M w_t^{(i)} = 1$. If the approximation is properly constructed, meaning that $p_M(r_{0:t}, \boldsymbol{\omega}_{0:t}, a_{0:t} | \mathbf{y}_{1:t}) \xrightarrow{M \rightarrow \infty} p(r_{0:t}, \boldsymbol{\omega}_{0:t}, a_{0:t} | \mathbf{y}_{1:t})$ in some adequate sense, then it is straightforward to use (7) in order to approximate any estimators of $r_{0:t}$ or r_t . In particular, since

$$\begin{aligned} p_M(r_t | \mathbf{y}_{1:t}) &= \sum_{a_{0:t}} \int_{\boldsymbol{\omega}_{0:t}} \int_{r_{0:t-1}} p_M(r_{0:t}, \boldsymbol{\omega}_{0:t}, a_{0:t} | \mathbf{y}_{1:t}) dr_{0:t-1} d\boldsymbol{\omega}_{0:t} \\ &= \sum_{i=1}^M \delta_i(r_t) w_t^{(i)}, \end{aligned} \quad (8)$$

where δ_i is the delta measure located at $r_t^{(i)}$, we readily calculate the (approximate) minimum mean square error (MMSE) estimate of r_t as

$$\hat{r}_t^{mmse} = \int r_t p_M(r_t | \mathbf{y}_{1:t}) dr_t = \sum_{i=1}^M r_t^{(i)} w_t^{(i)}. \quad (9)$$

¹Since we are interested in tracking r_t , the natural choice of our objective pdf of interest should have been $p(r_{0:t} | \mathbf{y}_{1:t})$. However, working with the latter marginal density leads to an exponential growth (with t) in the complexity of the SMC algorithm, unless some (not always well justified) approximations are used.

The generation of samples and the computation of weights is carried out by means of the importance sampling (IS) principle [9]. Let $\pi(r_{0:t}, \boldsymbol{\omega}_{0:t}, a_{0:t})$ denote a proposal pdf (often called *importance function* in the IS terminology) such that $\pi(r_{0:t}, \boldsymbol{\omega}_{0:t}, a_{0:t}) > 0$ whenever $p(r_{0:t}, \boldsymbol{\omega}_{0:t}, a_{0:t} | \mathbf{y}_{1:t}) > 0$. The proposal density is used to generate samples,

$$\left(r_{0:t}^{(i)}, \boldsymbol{\omega}_{0:t}^{(i)}, a_{0:t}^{(i)} \right) \sim \pi(r_{0:t}, \boldsymbol{\omega}_{0:t}, a_{0:t}), \quad i = 1, \dots, M, \quad (10)$$

and the associated weights are proportional to the ratio of the objective pdf over the importance function,

$$w_t^{(i)} \propto \frac{p(r_{0:t}^{(i)}, \boldsymbol{\omega}_{0:t}^{(i)}, a_{0:t}^{(i)} | \mathbf{y}_{1:t})}{\pi(r_{0:t}^{(i)}, \boldsymbol{\omega}_{0:t}^{(i)}, a_{0:t}^{(i)})}, \quad i = 1, \dots, M. \quad (11)$$

This procedure ensures the convergence of $p_M(r_{0:t}, \boldsymbol{\omega}_{0:t}, a_{0:t} | \mathbf{y}_{1:t})$ towards $p(r_{0:t}, \boldsymbol{\omega}_{0:t}, a_{0:t} | \mathbf{y}_{1:t})$, but it has little practical use because Eq. (10) implies that M complete sequences $r_{0:t}^{(i)}$, $\boldsymbol{\omega}_{0:t}^{(i)}$ and $a_{0:t}^{(i)}$, $i = 1, \dots, M$, must be drawn from the proposal at each time step, hence the computational complexity of the method grows with time.

Fortunately, the IS principle can be implemented *sequentially*, with a fixed complexity independent of time. A straightforward application of Bayes' theorem yields the recursive decomposition

$$\begin{aligned} &p(r_{0:t}, \boldsymbol{\omega}_{0:t}, a_{0:t} | \mathbf{y}_{1:t}) \propto \\ &p(\mathbf{y}_t | r_t) p(r_t | r_{0:t-1}, \boldsymbol{\omega}_{0:t-1}, a_{0:t-1}) p(a_t | a_{t-1}) \\ &\times p(\boldsymbol{\omega}_t | \boldsymbol{\omega}_{t-1}, a_{t-1}) p(r_{0:t-1}, \boldsymbol{\omega}_{0:t-1}, a_{0:t-1} | \mathbf{y}_{1:t-1}). \end{aligned} \quad (12)$$

Therefore, if we factorize the importance function as

$$\pi(r_{0:t}, \boldsymbol{\omega}_{0:t}, a_{0:t}) \propto \pi(r_t, \boldsymbol{\omega}_t, a_t) \pi(r_{0:t-1}, \boldsymbol{\omega}_{0:t-1}, a_{0:t-1}), \quad (13)$$

and substitute (12) and (13) into (11), then we obtain a recursive expression for the importance weights,

$$\begin{aligned} w_t^{(i)} &\propto \frac{p(\mathbf{y}_t | r_t) p(r_t | r_{0:t-1}, \boldsymbol{\omega}_{0:t-1}, a_{0:t-1})}{\pi(r_t, \boldsymbol{\omega}_t, a_t)} \\ &\times p(\boldsymbol{\omega}_t | \boldsymbol{\omega}_{t-1}, a_{t-1}) p(a_t | a_{t-1}) w_{t-1}^{(i)}. \end{aligned} \quad (14)$$

Moreover, (13) means that, at time t , we can draw

$$\left(r_t^{(i)}, \boldsymbol{\omega}_t^{(i)}, a_t^{(i)} \right) \sim \pi(r_t, \boldsymbol{\omega}_t, a_t), \quad i = 1, \dots, M, \quad (15)$$

and append the new samples to the existing streams, $r_{0:t-1}^{(i)}$, $\boldsymbol{\omega}_{0:t-1}^{(i)}$ and $a_{0:t-1}^{(i)}$ (which need not be modified), to build the sequences $r_{0:t}^{(i)}$, $\boldsymbol{\omega}_{0:t}^{(i)}$ and $a_{0:t}^{(i)}$. Eqs. (15) and (14) together yield a sequential IS (SIS) type of algorithm for the construction of $p_M(r_{0:t}, \boldsymbol{\omega}_{0:t}, a_{0:t} | \mathbf{y}_{1:t})$ [7].

It is well known, however, that the sequential application of (15) and (14) with a finite number of particles, $M < \infty$, quickly leads to a degenerate set of particles [7]. Indeed, the variance of the weights increases stochastically with time and, after a few time steps, one single particle tends to accumulate all the weight and the approximation $p_M(r_{0:t}, \boldsymbol{\omega}_{0:t}, a_{0:t} | \mathbf{y}_{1:t})$ becomes useless. This difficulty is commonly overcome by adding a resampling step [7] which, intuitively, consists in stochastically discarding the particles with low weights while the particles with higher weights are replicated. Although

several resampling schemes exist (and all of them can be plugged into the tracking algorithm without any added difficulty), in this paper we adopt the conceptually simple multinomial resampling method which can be interpreted as drawing a new set of M samples from the approximation $p_M(r_{0:t}, \omega_{0:t}, a_{0:t} | \mathbf{y}_{1:t})$, i.e., we let

$$\left(\tilde{r}_{0:t}^{(i)}, \tilde{\omega}_{0:t}^{(i)}, \tilde{a}_{0:t}^{(i)} \right) = \left(r_{0:t}^{(k)}, \omega_{0:t}^{(k)}, a_{0:t}^{(k)} \right), \quad \text{with probability } w_t^{(k)}, \quad (16)$$

for each $i = 1, \dots, M$ and $k \in \{1, \dots, M\}$. Then, the particles are renamed, $\left(r_{0:t}^{(i)}, \omega_{0:t}^{(i)}, a_{0:t}^{(i)} \right) \leftarrow \left(\tilde{r}_{0:t}^{(i)}, \tilde{\omega}_{0:t}^{(i)}, \tilde{a}_{0:t}^{(i)} \right)$, and the weights are reset, $w_t^{(i)} = \frac{1}{M}$ for all i (since we are drawing M i.i.d. samples from our current best approximation of the objective pdf). A resampling step can be taken every time the approximate effective sample size [7] $\hat{M}_{eff} = \frac{1}{\sum_{i=1}^M w_t^{(i)2}}$ falls below a user-defined threshold ($\hat{M}_{eff} \leq M$, hence typical threshold values are λM for some $0 < \lambda < 1$).

B. Evaluation of The Weights

In order to ensure that the weights can be computed, we must be able to evaluate the factors $p(a_t | a_{t-1})$, $p(\omega_t | \omega_{t-1}, a_{t-1})$, $p(r_t | r_{0:t-1}, a_{0:t-1})$ and $p(\mathbf{y}_t | r_t)$ in (14). The transition densities $p(a_t | a_{t-1})$ and $p(\omega_t | \omega_{t-1}, a_{t-1})$ are part of the model, hence known by assumption. The prior density of the position at time t , $p(r_t | r_{0:t-1}, a_{0:t-1}, \omega_{0:t-1})$, is Gaussian and can be obtained in closed form for each particle. Indeed, given $r_{0:t-1}^{(i)}$, $a_{0:t-1}^{(i)}$ and $\omega_{0:t-1}^{(i)}$, the system

$$\begin{bmatrix} v_t \\ r_t \end{bmatrix} = \mathbf{A}(\omega_{t-1}^{(i)}) \begin{bmatrix} v_{t-1} \\ r_{t-1}^{(i)} \end{bmatrix} + \mathbf{q}u_t \quad (17)$$

is linear and Gaussian, with known parameters, and all posterior pdf's, including $p(r_t | r_{0:t-1}^{(i)}, a_{0:t-1}^{(i)}, \omega_{0:t-1}^{(i)})$, are Gaussian and can be computed exactly using a Kalman filter [8], [6]. In the sequel, we will denote $p(r_t | r_{0:t-1}^{(i)}, a_{0:t-1}^{(i)}, \omega_{0:t-1}^{(i)}) = CN(r_t; \bar{r}_{t|t-1}^{(i)}, \sigma_{r_t}^{(i)2})$.

The pdf $p(\mathbf{y}_t | r_t)$ is usually referred to as the likelihood of r_t . If we write $p(y_{j,t} | r_t)$ as a marginal of the joint density $p(y_{j,t}, m_{j,t} | r_t)$, then it is straightforward to obtain the expression

$$p(\mathbf{y}_t | r_t) = \prod_{j=1}^J p(y_{j,t} | r_t) = \prod_{k=1}^J \sum_{m_{j,t}} p(y_{j,t} | r_t, m_{j,t}) p(m_{j,t}),$$

where both $p(y_{j,t} | r_t, m_{j,t}) = N(y_{j,t}; f_{m_{j,t}}(r_t), \sigma_{\epsilon}^2)$ and $p(m_{j,t})$ are known from the model, for all $j = 1, \dots, J$.

C. Importance Function

A good deal of the performance of the proposed algorithm depends on the choice of the importance function. The simplest choice is the prior

$$\pi(r_t, a_t, \omega_t) = p(r_t | r_{0:t-1}, a_{0:t-1}, \omega_{0:t-1}) p(a_t | a_{t-1}) p(\omega_t | \omega_{t-1}), \quad (18)$$

which reduces the importance weight calculation to $w_t^{(i)} \propto w_{t-1}^{(i)} p(\mathbf{y}_t | r_t^{(i)})$. More sophisticated importance functions can lead to more efficient algorithms, though. For instance, if

- 1) Initialization, at $t = 0$:
 - For $i = 1, \dots, M$, draw a_0 , ω_0 and r_0 from the priors $p(r_0)$, $p(\omega_0)$ and $p(a_0)$, respectively. Set $w_0^{(i)} = \frac{1}{M}$.
- 2) Recursive step, for $t > 0$:
 - For $i = 1, \dots, M$, draw $a_t^{(i)} \sim p(a_t | a_{t-1}^{(i)})$, $\omega_t^{(i)} \sim p(\omega_t | \omega_{t-1}^{(i)}, a_{t-1}^{(i)})$ and $r_t^{(i)} \sim p(r_t | r_{0:t-1}^{(i)}, \omega_{0:t-1}^{(i)}, a_{0:t-1}^{(i)})$.
 - For $i = 1, \dots, M$, update the weights, $w_t^{(i)} \propto w_{t-1}^{(i)} p(\mathbf{y}_t | r_t^{(i)})$.
 - Find the effective sample size $\hat{M}_{eff} = 1 / \sum_{k=1}^M w_t^{(k)2}$. If $\hat{M}_{eff} < \lambda M$ then resample.

TABLE I

RAO-BLACKWELLIZED PARTICLE FILTER FOR THE GIMM SYSTEM.

at time t we compute estimates $\hat{m}_{j,t}^{(i)}$ (e.g., MAP or maximum likelihood estimates are relatively easy to obtain), then we can linearize the observation functions $f_{\hat{m}_{j,t}^{(i)}}$ and analytically find a Gaussian approximation of the posterior $p(r_t | \mathbf{y}_t, r_{0:t-1}^{(i)}, a_{t-1}^{(i)}, \omega_{t-1}^{(i)}) \approx CN(r_t; \tilde{r}_t^{(i)}, \tilde{\sigma}^{(i)2})$, where the mean $\tilde{r}_t^{(i)}$ and variance $\tilde{\sigma}^{(i)2}$ can be obtained by taking the prediction and update steps of an extended Kalman filter.

D. Summary

Table I shows a summary of the proposed Rao-Blackwellized SMC tracking algorithm, with prior importance function, for the GIMM state-space model.

IV. SIMULATION AND EXPERIMENTAL RESULTS

A. Experimental setup and state-space models

We have carried out experiments in a network consisting of six nodes located at fixed positions, acting as RSS sensors, and one extra node acting as the moving target. The nodes are ZigBee motes, each one consisting of a small circuit board with its own processor and a transmission system based on the IEEE 802.15.4 standard and upper layers defined by the ZigBee Alliance. Two type of motes have been used, including Crossbow and a combination of Arduino microprocessors with Xbee chipsets. The RSS for any transmission between motes is easily extracted from any of the two nodes. The network consisted of six motes deployed in an area of 6×10 meters, in the positions (0,0), (6,0), (0,5), (6,5), (0,10) and (6,10) meters.

In order to select the observation functions $f_k(r_t)$, $k = 1, \dots, K$, for this scenario we collected a large number ($\approx 150,000$) of RSS measurements associated to 28 different distances, d_1, \dots, d_{28} , between a minimum of $d_1 = 0$ m and a maximum of $d_{28} = 12$ m. From these data, we constructed a histogram for each different distance. As an example, Fig. 1 shows the results for $d_1 = 0$, $d_2 = 1$, $d_3 = 2$ and $d_6 = 3$. Each histogram shows the range (x-axis) and frequency (y-axis) of the RSS measurements (in dB) collected by the sensors, grouped in bins of 1 dB. It is apparent that the histograms are *not* unimodal. Therefore, a multimodal representation of the observations, such as the one in the proposed GIMM model, is necessary indeed.

The simplest possible GIMM model is obtained when taking $L = 1$ and $K = 2$. The reason to use a single dynamic

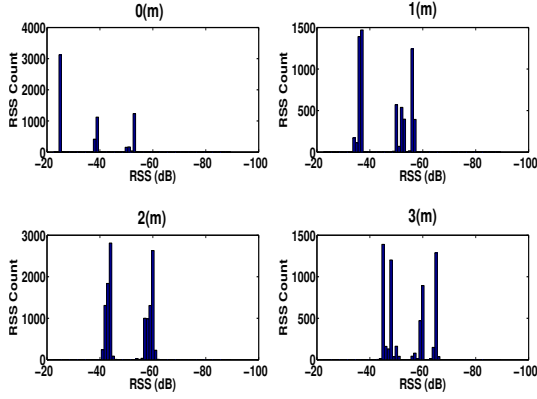


Fig. 1. Histograms displaying the absolute frequency of the RSS observations versus their range (in dB). The histograms are related to distances (from left to right and top to bottom) $d_1 = 0$, $d_2 = 1$, $d_3 = 2$ and $d_6 = 3$ m.

model in this example² is that classical IMM schemes, where $L > 1$ motion models are applied, have been reported to work properly in the general maneuvering target tracking literature and, more specifically, using particle filters [5]. Therefore, the relevant goal is to assess the ability of the Rao-Blackwellized particle filter to switch between measurement models. In order to construct the $K = 2$ models, we have:

- 1) Used the k -means algorithm to separate the observations, for each distance d_i , $i = 1, \dots, 28$, into two clusters. This is straightforward for some distances, but it is apparent that the data exhibit more than two modes for several values of i . Let $S_{i,1}$ and $S_{i,2}$ be the observation clusters for distance d_i and models 1 and 2, respectively.
- 2) Computed the sample mean for each cluster and each distance, denoted $\mu_{i,1}$ and $\mu_{i,2}$ for distance d_i and models 1 and 2, respectively. Similarly, we have obtained sample variances $\sigma_{i,1}^2$ and $\sigma_{i,2}^2$.
- 3) Fitted two polynomials of degree 6, $g_1(d) = \sum_{i=0}^6 \alpha_{1,i} d^i$ and $g_2(d) = \sum_{i=0}^6 \alpha_{2,i} d^i$, to the experimentally obtained sequences of sample means $\mu_{1,1}, \dots, \mu_{28,1}$ and $\mu_{1,2}, \dots, \mu_{28,2}$, respectively, for models 1 and 2. Similarly, we have fitted degree 6 polynomials, $h_1(d) = \sum_{i=0}^6 \beta_{1,i} d^i$ and $h_2(d) = \sum_{i=0}^6 \beta_{2,i} d^i$, for the sample variances, $\sigma_{1,1}^2, \dots, \sigma_{28,1}^2$ and $\sigma_{1,2}^2, \dots, \sigma_{28,2}^2$. The polynomial coefficients, $\{\alpha_{k,i}\}_{i=0}^6$ and $\{\beta_{k,i}\}_{i=0}^6$, with $k = 1, 2$, have been selected by a least squares procedure.

With these elements, a preliminary choice of the observation function for the k -th model and the j -th sensor is $f_k(r_t) = g_k(d_{j,t})$, where $d_t = |r_t - s_j|$ is the distance between the target position, r_t , and the j -th sensor location, s_j , while the observation noise is Gaussian with zero mean and variance $h_k(d_{j,t})$. The polynomials $g_1(d)$ and $g_2(d)$, together with the points from which they are fitted, are shown in Fig. 2 left and right, respectively. The polynomials $h_1(d)$ and $h_2(d)$ are shown in Fig. 3 left and right, respectively.

²We have used the simplest possible model, given by Eq. (1), even if this is clearly not the best representation of the kind of motion considered in the experiment. We believe that a careful choice of the dynamic model will further improve the performance of the tracker.

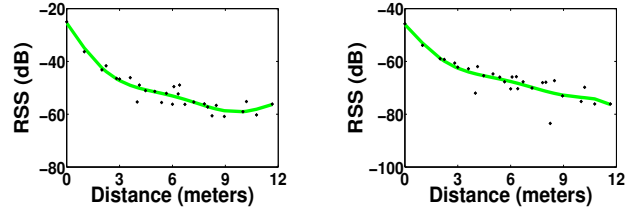


Fig. 2. Polynomials $g_1(d)$ (left) and $g_2(d)$ (right) describing the fitted mean of the RSS measurements versus distance. The points show the experimental data used for fitting the functions

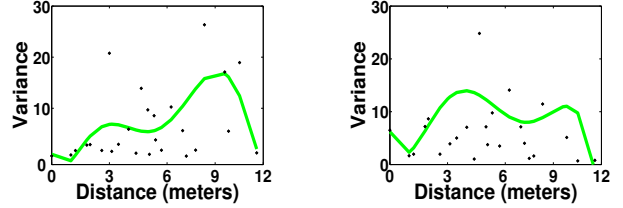


Fig. 3. Polynomials $h_1(d)$ (left) and $h_2(d)$ (right) describing the fitted variance of the RSS measurements versus distance. The points show the experimental data used for fitting the functions.

Unfortunately, the experimental data show that the RSS observations become highly unreliable when the distance between the target and the sensor is large (see the large fluctuations of the data points, for $d > 3$, in Figs. 2 and 3). Therefore, the straightforward choice of the likelihood,

$$p(y_{j,t}|r_t, m_{j,t}) = N(y_{j,t}; g_{m_{j,t}}(d_{j,t}), h_{m_{j,t}}(d_{j,t})), \quad (19)$$

turns out of little use. Better results are obtained if we relate the RSS observations to distances, using (19), when the received power is large enough, but assign a distance-independent likelihood value otherwise. Specifically, we *define* the likelihood function

$$p(y_{j,t}|r_t, m_{j,t}) \triangleq N(y_{j,t}; g_{m_{j,t}}(d_{j,t}), h_{m_{j,t}}(d_{j,t})) (1 - \Phi_{m_{j,t}}(\gamma_{m_{j,t}})) + N(y_{j,t}; \hat{\mu}_{m_{j,t}}, \hat{\sigma}_{m_{j,t}}^2) \Phi_{m_{j,t}}(\gamma_{m_{j,t}}), \quad (20)$$

where $\Phi_{m_{j,t}}(\gamma) = \int_{-\infty}^{\gamma} N(y; g_{m_{j,t}}(d_{j,t}), h_{m_{j,t}}(d_{j,t})) dy$. The RSS thresholds are set to $\gamma_1 = -46$ dB and $\gamma_2 = -60$ dB and the distance-independent mean and variance parameters for the two models, $\hat{\mu}_k$ and $\hat{\sigma}_k^2$, for $k = 1, 2$, respectively, are also fitted to the experimental data.

B. Computer Simulation Results

In order to illustrate the performance of the proposed method in a controlled scenario, we have selected two regular trajectories for the target and generated synthetic observations by drawing them from (20). Then, we have applied the Rao-Blackwellized particle filter (RBPF) to track the target. The complete set of simulation and algorithm parameters is listed in Table IV-B.

Figure 4 shows the reference trajectories (solid black lines), the estimates provided by the RBPF in a single simulation run (solid red lines) and the location of the sensors (blue points). When averaged over 100 simulations, the mean absolute error (MAE) in the estimation of the target position for the trajectory in Figure 4-left is $\text{MAE} = 1.5623$ m, with a standard deviation of 1.372 m. The corresponding MAE

Parameter	Value
Total no. of particles, M	2000
Resampling threshold, λ	0.2
Total no. of sensors, J	6
Total simulation time, trajectory 1, T_1	52.2 s
Total simulation time, trajectory 2, T_2	50.2 s
Sampling period, T_s	0.2 s
Threshold for model 1, γ_1	-46 dB
Threshold for model 2 γ_2	-60 dB
State Equation noise variance, σ_u^2	0.7
Probability for model 1, $p(m_{i,t} = 1)$	0.5
Probability for model 2, $p(m_{i,t} = 2)$	0.5

TABLE II
PARAMETERS OF SIMULATION

and standard deviation for the trajectory in Figure 4-right are 1.7347 m and 1.373 m, respectively. We have also simulated a random trajectory with a duration of 5 minutes in the described area of 6×10 . For this simulation we used a mesh of 12 sensors holding up the positions (0,0), (3,0), (6,0), (0,3), (3,3), (6,3), (0,6), (3,6), (6,6), (0,9), (3,9) and (6,9) meters. The averaged MAE over 100 simulations was 0.4531 m and the standard deviation was 0.7314 m.

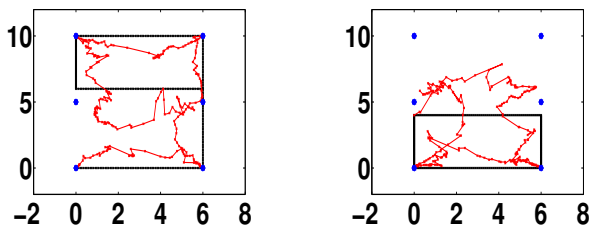


Fig. 4. Results of target tracking with two reference trajectories and synthetic observations generated according to Eq. (20). The true trajectories are plotted in solid black lines, the estimates in solid red lines and the sensors are shown by blue points.

C. Experimental results

Since our main goal is the experimental verification of the validity of the GIMM scheme and the RBPF, we have also applied the same tracking algorithm (with exactly the same parameters) to the estimation of the same two reference trajectories using experimentally collected data. The measurements were obtained with the same setup described in Section IV-A, but independently from the observations used to fit the model.

Figure 5 shows the obtained results. They are satisfactory, in the sense that the error is similar to the one achieved when the observations are synthetic.

V. CONCLUSIONS

We have proposed a generalized interacting multiple-model (GIMM) approach to the representation of the target dynamics and the radio signal-strength (RSS) observations in an indoor scenario. The resulting class of state-space models is very flexible and we claim it may enable the adequate formal representation of time-varying scenarios with highly unstable RSS measurements. The drawback of the GIMM system is the increase in the dimension of the system state that must be tracked. To handle this difficulty, we have introduced a

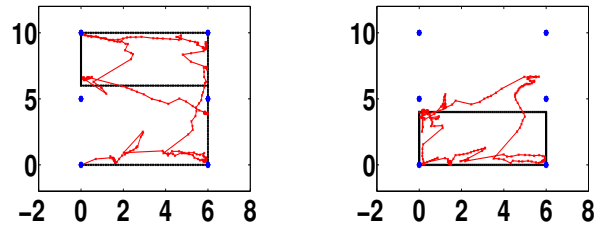


Fig. 5. Results of target tracking with two reference trajectories and experimental observations. The true trajectories are plotted in solid black lines, the estimates in solid red lines and the sensors are shown by blue points.

Rao-Blackwellized particle filter that jointly estimates the target trajectory and the additional state variables needed to represent the interacting models. We have provided numerical results that illustrate the performance of the proposed method with both synthetic and experimental RSS measurements.

VI. ACKNOWLEDGMENTS

The authors acknowledge the support of *Centro para el Desarrollo Tecnológico e Industrial* (CDTI) through project TIMI (ref. CEN-2002-2007). K. A., L. M. and J. M. acknowledge the support of *Ministerio de Ciencia e Innovación* (project MONIN, ref. TEC-2006-13514-C02-01/TCM and program CONSOLIDER-INGENIO 2010, ref. CSD2008-00010 COMONSENS) and *Comunidad de Madrid* (project PROMULTIDIS-CM, ref. S-0505/TIC/0233). J. R. and C. J. E. acknowledge the support of *Xunta de Galicia* (project no. 07TIC019105PR) and *Ministerio de Industria, Turismo y Comercio* (project ref. TSI-020301-2008-2).

REFERENCES

- [1] N. Patwari, J. N. Ash, S. Kyperountas, A. O. Hero III, R. L. Moses, and N. S. Correal, "Locating the nodes," *IEEE Signal Processing Magazine*, vol. 22, no. 4, pp. 54–69, July 2005.
- [2] F. Gustafsson and F. Gunnarsson, "Mobile positioning using wireless networks," *IEEE Signal Processing Magazine*, vol. 22, no. 4, pp. 41–53, July 2005.
- [3] T. S. Rappaport, *Wireless Communications: Principles and Practice (2nd edition)*, Prentice-Hall, Upper Saddle River, NJ (USA), 2001.
- [4] A. Doucet, N. de Freitas, and N. Gordon, Eds., *Sequential Monte Carlo Methods in Practice*, Springer, New York (USA), 2001.
- [5] S. McGinnity and G. W. Irwin, "Manoeuvring target tracking using a multiple-model bootstrap filter," in *Sequential Monte Carlo Methods in Practice*, A. Doucet, N. de Freitas, and N. Gordon, Eds., chapter 23, pp. 479–496. Springer, 2001.
- [6] F. Gustafsson, F. Gunnarsson, N. Bergman, U. Forssell, J. Jansson, R. Karlsson, and P.-J. Nordlund, "Particle filters for positioning, navigation and tracking," *IEEE Transactions Signal Processing*, vol. 50, no. 2, pp. 425–437, February 2002.
- [7] A. Doucet, S. Godsill, and C. Andrieu, "On sequential Monte Carlo Sampling methods for Bayesian filtering," *Statistics and Computing*, vol. 10, no. 3, pp. 197–208, 2000.
- [8] R. Chen and J. S. Liu, "Mixture Kalman filters," *Journal of the Royal Statistical Society B*, vol. 62, pp. 493–508, 2000.
- [9] M. H. DeGroot and M. J. Schervish, *Probability and Statistics, 3rd ed.*, Addison-Wesley, New York, 2002.